The paper was published in the proceedings of the 9th International Symposium on Geotechnical Aspects of Underground Construction in Soft Ground (IS – Sao Paulo 2017) and was edited by Arsenio Negro and Marlísio O. Cecílio Jr. The conference was held in Sao Paulo, Brazil in April 2017.

Geotechnical Aspects of Underground Construction in Soft Ground – Negro & Cecilio Jr. (Eds)
© 2018 Taylor & Francis Group, London, ISBN 978-1-138-29711-1

K_0 parameter influence in tunneling superficial settlements and in liner stresses

V. Armigliato, A.C.G. da Silva & C.M.A. Prado
Arcadis Logos, São Paulo, Brazil

ABSTRACT: This paper describes the influence of the k_0 parameter (ratio between vertical and horizontal "in situ" stresses) in superficial settlements and liner stresses caused by NATM tunnel excavation in a residual soil massif in São Paulo Line 4 Yellow Subway expansion. Are presented two-dimensional numerical analyses using Finite Diferences Method implemented in FLAC software, for the construction method simulation. The soil behavior is simulated by Linear Elastic model with Mohr-Coulomb envelope.

1 INTRODUCTION

One of the most important geotechnical parameters in tunnel excavation numerical simulation is the in situ ratio between vertical and horizontal stresses (k_0). Its importance in settlements prediction and liner design has been research object of several engineers.

Although its value determines significantly the numerical excavation simulations results, it is, in most cases, estimated by empirical correlations published such Jaky (1944) and Mayne and Kulhawy (1982).

In fact, the in situ ratio k_0 is a value of difficult practical determination, in field or in laboratory, been almost impossible its determination in laboratory, when regarding to residual soils (Pinto and Nader, 1991).

This paper presents numerical analyses performed for a circular tunnel with cover varying from one to two times the tunnel diameter. It is discussed the influence of the parameter k_0 in the prediction of the settlements at ground surface and also the effects on the liner design of the tunnel. For that five k_0 values were chosen, which are: 0.5, 0.7, 1.0, 1.5 and 2.0 and the graphics show the settlements on the ground surface, the axial force and the bending moment on the liner.

2 OUTLINE OF NUMERICAL ANALYSIS

2.1 *Modeling of soil, lining and tunnel excavation process*

The Figure 1 shows the boundary conditions and the finite differences grid used in the analysis for the tunnel cover, which is equal to one time the tunnel diameter. The bi-dimensional Finite Differences Method used is implemented in ITASCA FLAC 7.0 code.

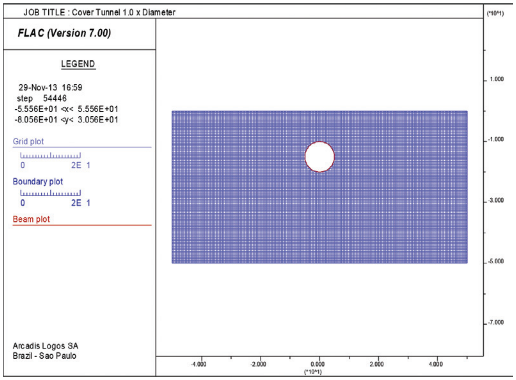

Figure 1. Finite differences grid.

Table 1. Properties of Soil Massif.

Density (10^3kg/m^3)	1.8
Poisson's ratio	0.2
Cohesion (kPa)	18–0.010
Friction angle (degree)	30
Elastic Modulus (MPa)	40
Coefficient of earth pressure at rest, k_0	0.5;0.7;1.0;1.5;2.0

The soil massif were simulated using two rheological behavior: (1) linear elastic and (2) elastic perfectly plastic model using Mohr Coulomb envelope. The Table 1 shows the parameters of the soil models used in the analyses.

The liner of the tunnel was simulated with beam elements that have perfect linear elastic behavior,

Table 2. Analysis procedure.

Phase	Construction Process
Phase 0	Initial conditions
Phase 1	50% Stress Relief
Phase 2	Excavation and Liner Application

30 cm thickness and Young Modulus equal to GPa to simulate the liner loading in early shotcrete ages and Poisson Coefficient 0.2.

The tunneling simulation used a 50% stress relief technique to simulate the tri-dimensional effect of the face. The sequence is shown in Table 2.

3 ANALYSES RESULTS

3.1 *Axial forces in liner*

The Figure 2 shows the variation of the axial force in the liner in function of the k_0 variation, for the different tunnel covers 1D, 1.5D and 2.0D respectively for the elastic simulations.

A similar behavior is observed in Figures 3 and 4, which shows the results for elastic-plastic simulations. Additionally, it's noticed that the axial force isn't influenced for the cohesion value.

In these figures it is observed that for two points in the liner at 0° and 180° (crown apex and invert), happens an axial force increase while the k_0 value increases from 0.5 to 2.0. For the points situated et 90° and 270° (walls) there are no variation of the axial force in function of the k_0 value variation.

3.2 *Analyses of the bending moments*

The bending moment diagrams vary in function of the tunnel cover. The Figure 5 shows the distribution of the bending moments for the covers of 1.0D, 1.5D and 2.0D, respectively, considering the elastic behavior for the soil massif.

It's observed in the Figure 5 that for $k_0 = 1$ the bending moment in the tunnel perimeter, from 0° to 360°, is not a function of the cover. However, for $k_0 < 1$, considering the two places 0°±45° and 180°±45°, it's noticed that the bending moment has negative sign, indicating for the sign convention that the extern fiber of the liner are compressed in this place. It's observed that as the k_0 increases the value of the module of the moment decreases, being equal to zero for $k_0 = 1$, as it was observed before.

Still for $k_0 < 1$, the places between 90°±45° and 270°±45° shows positive bending moment, indicating that the extern fibers are tensioned in this place. In the same way, as k_0 increases the bending moment decreases, approaching zero when the k_0 is close to 1.

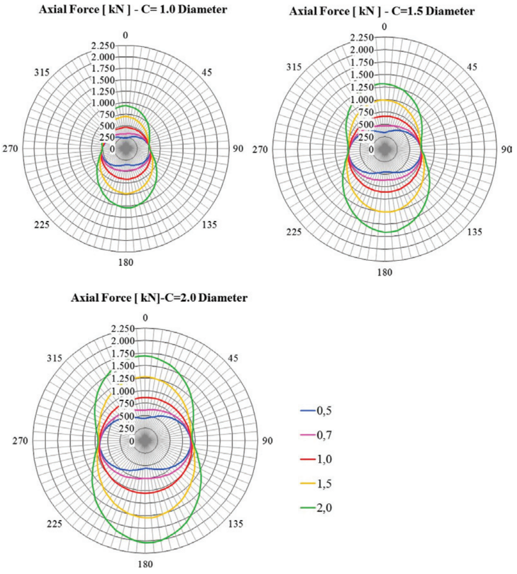

Figure 2. Axial forces—linear elastic model.

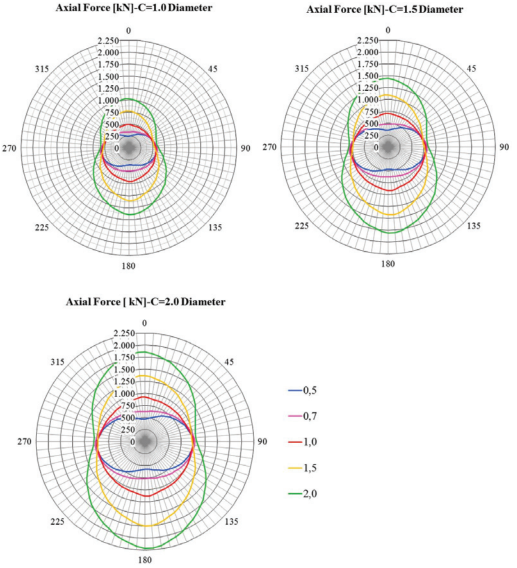

Figure 3. Axial force—Mohr-Coloumb envelope. cohesion = 18 kPa.

The points at 45°, 135°, 225° and 315° are inflection points for the bending moment diagrams.

For $k_0 > 1$ the places 0°±45° and 180°±45° show positive bending moments indicating that, in opposition to what happen for $k_0 < 1$, in this place the outer fibers are tensioned, increasing as the k_0 increases.

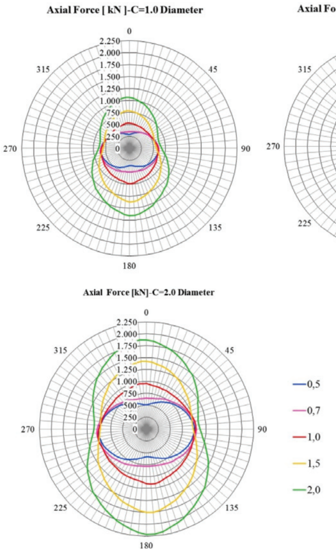

Figure 4. Axial force—Mohr-Coloumb envelope. cohesion = 10 Pa.

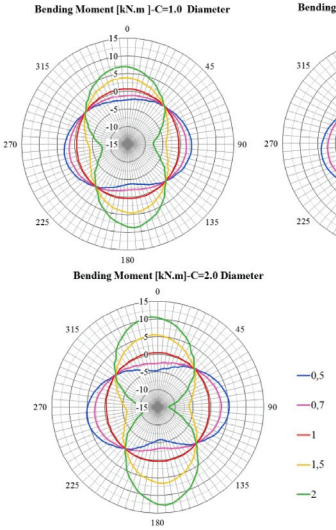

Figure 5. Bending moments—linear elastic model.

For the $k_0 > 1$, in the places 90°±45° and 270° ± 45° the bending moment is negative indicating the outer fiber compression.

As the k_0 increases, the absolute value of bending moment increases.

It is a conclusion that the magnitude of k_0 has influence in the liner location subjected to tension or compression.

In the Figures 6 and 7 are shown the results of the analyses in the elastic plastic regime, with c = 18 kPa and c = 10 Pa, respectively.

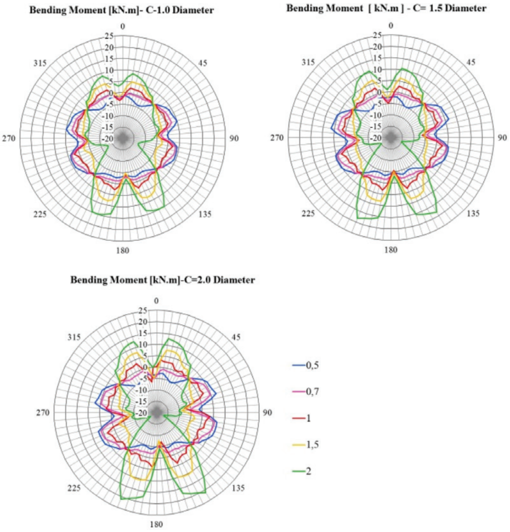

Figure 6. Bending moment—Mohr-Coloumb envelope, cohesion = 18 kPa.

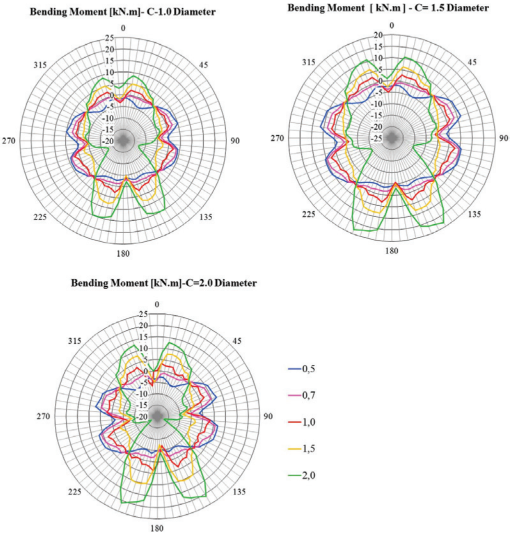

Figure 7. Bending moment—Mohr-Coloumb envelope, cohesion = 10 Pa.

The Figures 5, 6 and 7, show that the rheological model adopted to represent the soil behavior also influences in the shape of the bending moments diagram. However, comparing just the Figures 6 and 7, which represent the results of the analyses varying the magnitude of cohesion (18 kPa and 10 Pa), it's possible to conclude that the cohesion doesn't have influence in the value of the bending moment. It's observed that at 15°, 155°, 205° and

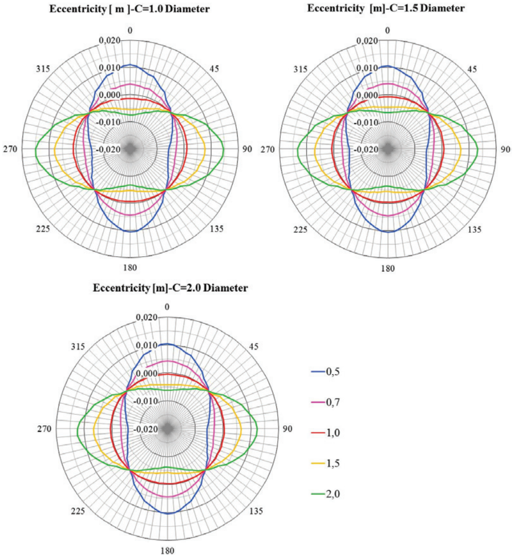

Figure 8. Eccentricity—linear elastic model.

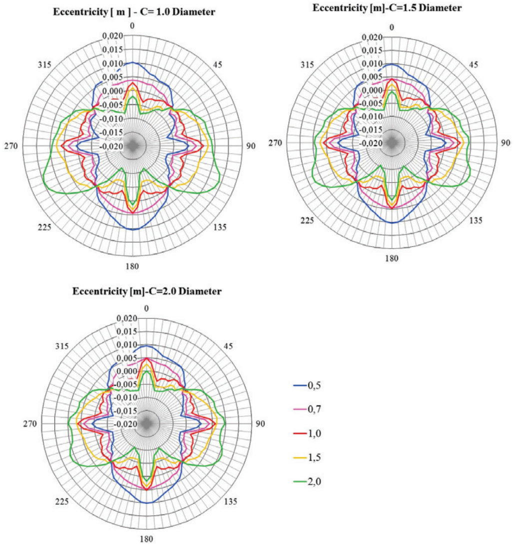

Figure 9. Eccentricity—Mohr Coloumb model cohesion = 18 kPa.

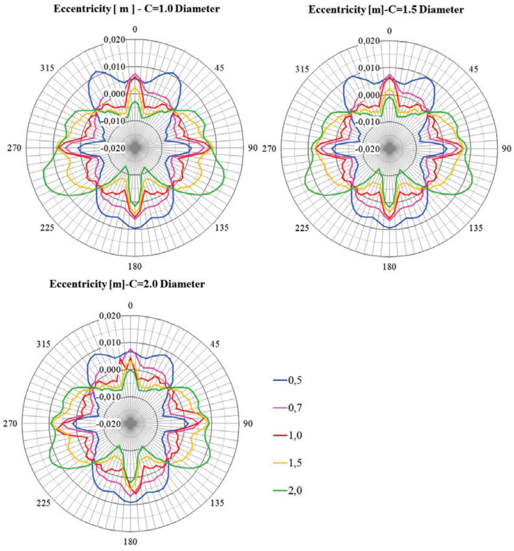

Figure 10. Eccentricity—Mohr Coloumb Model. cohesion = 10 Pa.

335° degrees the values of the bending moment diverge in less than 1,5% of the results of the analysis represented in the Figure 5 with those presented in the analyses of the Figure 6. This pattern of behavior is reproduced for all the analyses with the cover varying from 1.0D, 1.5D and 2.0D.

It was noticed that with the elastic plastic rheology more tensioned or compressioned regions are developed instead of the four previously described in Figure 5 (elastic behavior).

The Figures 6 and 7 show that, for $k_0 < 1$, the regions 0°±45° and 180°±45° have negative values, indicating compression in outer fibers.

3.4 *Surface settlement and gauss curves*

It is well know that the tunnel excavation causes stress relief around the excavation which conducts to superficial ground movements.

The shape of surface subsidence and its superficial settlements could be approximated with certain confidence through mathematical modelling. With this models, it's possible to obtain performance indicators that allow the knowledge of the massif stability conditions during the tunnel excavation.

Estimation of performance parameters values, helps on antecipating the damages that could occur on buildings or utilities present in the excavation influence zone area.

To define tunnels performance parameters, parametric curves are commonly used. Among numerous curves, the Gaussian is frequently used, as it leads to ease evaluation of tunneling performance such excavation volume loss, settlement basin definition or maximum differential settlement.

But the shape of the surface settlements obtained in the simulations carried out shown a different condition. Figures 11, 12 and 13 show the settlement profile for elastic behavior materials,

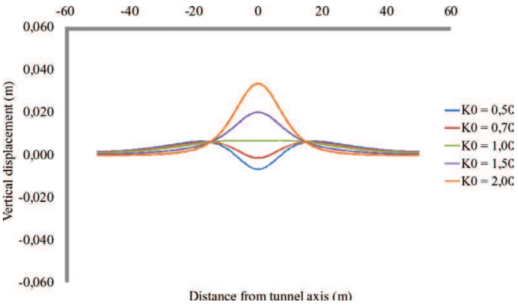

Figure 11. Settlement profiles for cover equal to the tunnel diameter for an elastic behavior material.

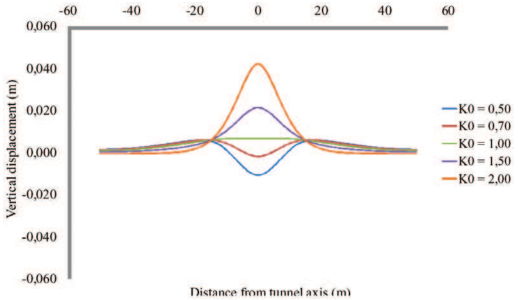

Figure 12. Settlement profiles for cover equal to 1.5D for a plastic elastic (Mohr Coulomb) behavior material.

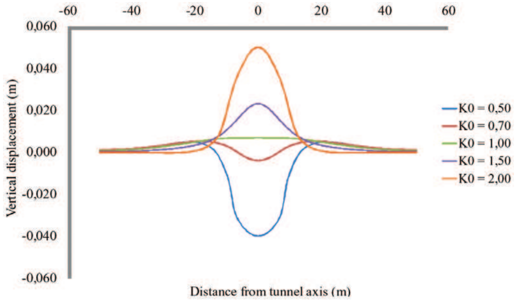

Figure 13. Settlement profiles for cover equal 2D for a low cohesion Mohr Coulomb behavior material.

plastic elastic (Morh Coulomb), and low-cohesion plastic elastic (low-cohesion Morh Coulomb).

With each numerical simulation, it was interpolated a Gauss curve to vertical displacement values. To define the proximity (or adherence) accuracy/degree between FLAC obtained points with the Gauss curve points, was used the coefficient of determination (R^2) that shows how much the Gaussian is close from numerical simulation values.

To rate the quality from the adjusts made, was adopted the following criteria, using the determination coefficients (R^2):

a. For values in which R^2 adjustment are higher than 0,95, was rated as good adherence adjustment ($R^2 > 0{,}95$)
b. For values in which R^2 adjustment are between 0,95 and 0,80, was rated as medium adherence adjustment ($0{,}95 < R^2 \leq 0{,}80$);
c. For values in which R^2 adjusment is lower than 0,80, was rated as low adherence adjustment ($R^2 < 0{,}80$).

With the classification made according the adopted criteria, all analysis were separated in groups with the same k_0 interval. Table 3 shows analysis percentage and adjustment quality in different k_0 intervals.

Figures 14 to 20 express the result showed on Table 3, where the blue points represents the numerical analysis vertical displacement values and the black curve represents the adjusted Gaussian.

From the obtained data, as shown on Figures 14 to 22 as well on Table 3, can be viwed the adherence degree between the Settlement

Table 3. Percentual simulations adjustment quality.

Model	Adjustment quality	$K_0 < 1$ (%)	$K_0 = 1$ (%)	$K_0 > 1$ (%)
Elastic	High Adherence	50	33	17
	Medium Adherence	50	67	67
	Low Adhenrece	0	0	17
Morh Coulomb	High Adherence	50	33	50
	Medium Adherence	50	33	33
	Low Adhenrece	0	33	17
Morh Coulomb —Low Cohesion	High Adherence	33	67	33
	Medium Adherence	67	0	50
	Low Adhenrece	0	33	17

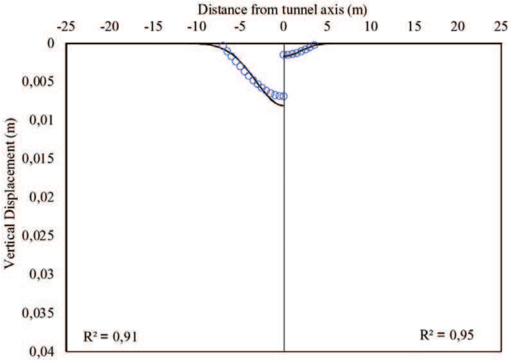

Figure 14. Gauss curve adjustment with points from the numerical model and elastic behavior for $K_0 < 1$.

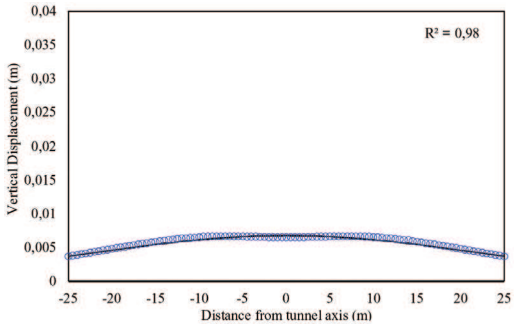

Figure 15. Gauss curve adjustment with points from the numerical model and elastic behavior for $K_0 = 1$.

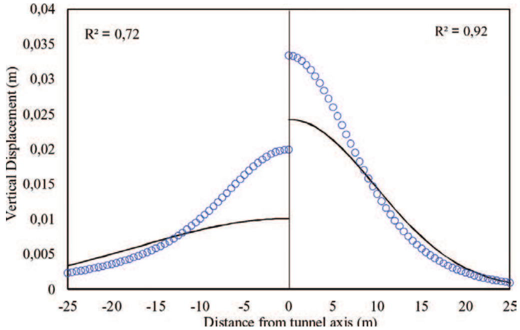

Figure 16. Gauss curve adjustment with points from the numerical model and elastic behavior for $K_0 > 1$.

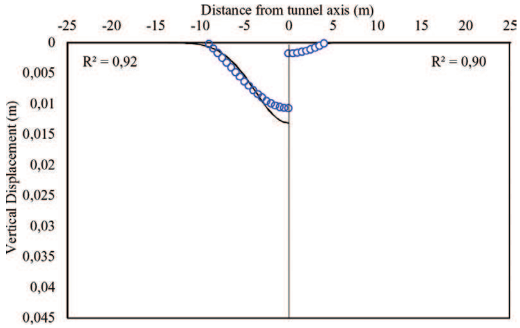

Figure 17. Gauss curve adjustment with points from the numerical model and plastic elastic (Morh Couloumb) behavior for $K_0 < 1$.

profile provided by the software and the interpolation with Gaussian and its direct relation with k_0. It can be noted that, for k_0 magnitudes below 1, the determination coefficient between the points that defines the settlement profile and the ones that outline Gauss curve, reaches satisfactory values regardless of the covering values. In all cases the analysis represented high and medium adherence adjustments, and in any case there was a low adherence.

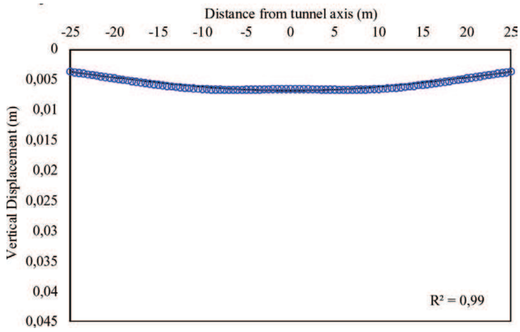

Figure 18. Gauss curve adjustment with points from the numerical model and plastic elastic (Morh Couloumb) behavior for $K_0 = 1$.

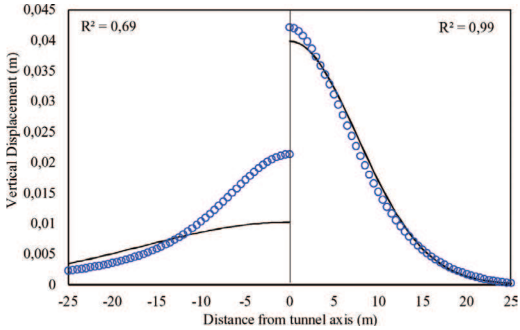

Figure 19. Gauss curve adjustment with points from the numerical model and plastic elastic (Morh Couloumb) behavior for $K_0 > 1$.

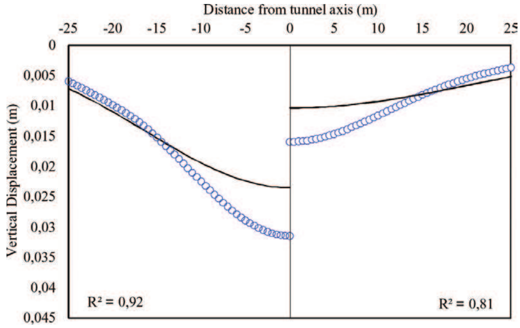

Figure 20. Gauss curve adjustment with points from the numerical model and low cohesion plastic elastic (low cohesion Morh Couloumb) behavior for $K_0 < 1$.

Despite the results obtained from k_0 equal or higher than 1 not being completely unsatisfactory,

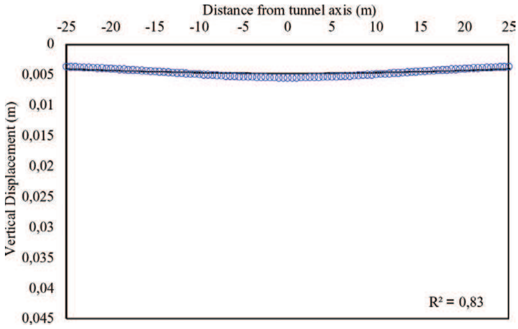

Figure 21. Gauss curve adjustment with points from the numerical model and low cohesion plastic elastic (low cohesion Morh Couloumb) behavior for $K_0 = 1$.

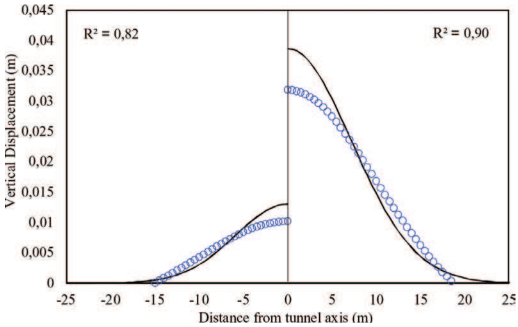

Figure 22. Gauss curve adjustment with points from the numerical model and low cohesion plastic elastic (low cohesion Morh Couloumb) behavior for $K_0 > 1$.

there were cases in which the reliability of data interpolation wasn't safe enough because some simulations showed low adherence adjustments. For $k_0 = 1.0$, the influence of the cover values over the adjustment is noted. In all cases, it is noted the difference between the percentage of all models used and the adjustment quality.

4 CONCLUSIONS

In this paper was presented a series of numerical simulations to analyse the influence of the paramenter k_0 in tunnel design. As it is a vast field of research, it was focused in evaluate the behavior of a circular sallow tunnel varying a few analyses paramenters.

The values of k_0 greater than one is not common when dealing with low overconsolidated sedimentary soils, when gravity is the main force, but is frequent in residual soils such São Paulo Pre Cambrians (Pinto and Nader, 1991, Queiroz et al, 2005), when chemical or tectonic forces prevail.

It was found that the Gaussian adjustment is poor to anticipate the settlements when dealing with massifs with k_0 greater than one and its derived tunneling performance parameters shall be poor as well.

Moreover the correct estimation of k_0 is fundamental to correct design of tunnel liner, as it could be compressed or tensioned as a function of it. So it is important, due to the difficult of k_0 estimative, that the design of concrete liner takes this aspect in account.

REFERENCES

Assis, A.; Celestino, T.B.; Koshima, A. and Telles, R.C.D. 2006. Tunnelling in Brazil. Sao Paulo: CBT/ABMS. 327p.

Celestino, T.B.; Rocha, H.C. and Nunes, N.L. 2007. Shotcrete in Brazil. Tunnels & Tunnelling, v.1, pp. 35–37.

Jaky J. (1948) Pressure in soils, 2nd ICSMFE, London, Vol. 1, pp. 103–107.

Mayne, P.W. and Kulhawy, F.H. (1982). "K_0-OCR relationships in soil". Journal of Geotechnical Engineering, Vol. 108 (GT6), 851–872.

Negro, A. 1988. Design of Shallow Tunnels in Soft Ground. Thesis (PhD in Civil Engineering)—University of Alberta. Alberta, 1480p.

Pinto, C.S.; Nader, J.J. Ensaios de laboratório em solos residuais, 2o Seminário de Engenharia de Fundações Especiais, São Paulo, 1991. Anais, v. 2, pp. 166–202.

Queiroz, P.I.B.; Roure, R.N and Negro, A. 2005. Bayesian updating of tunnel performance for K_0 estimate of Santiago gravel. In: Proceedings of the International Symposium on Geotechnical Aspects of Underground Construction in Soft Ground. Amsterdam: CRC Press/Balkema. pp. 211–218.